Radiation-induced magnetotransport in high-mobility two-dimensional systems: Role of electron heating

X. L. Lei and S. Y. Liu
Department of Physics, Shanghai Jiaotong University, 1954 Huashan Road, Shanghai 200030, China
(Received 28 February 2005; revised manuscript received 25 May 2005; published 17 August 2005)

Effects of microwave radiation on magnetoresistance are analyzed in a balance-equation scheme that covers regimes of inter- and intra-Landau level processes and takes into account photon-asissted electron transitions as well as radiation-induced change of the electron distribution for high-mobility two-dimensional systems. Short-range scatterings due to background impurities and defects are shown to be the dominant direct contributors to photoresistant oscillations. The electron temperature characterizing the system heating due to irradiation is derived by balancing the energy absorption from the radiation field and the energy dissipation to the lattice through realistic electron-phonon couplings, exhibiting resonant oscillation. Microwave modulations of the Shubnikov–de Haas oscillation amplitude are produced together with microwave-induced resistance oscillations, in agreement with experimental findings. In addition, the suppression of the magnetoresistance caused by low-frequency radiation in the higher magnetic field side is also demonstrated.

DOI: 10.1103/PhysRevB.72.075345 PACS number(s): 73.50.Jt, 73.50.Mx, 78.67.−n, 78.70.−g

I. INTRODUCTION

The discovery of microwave-induced magnetoresistance oscillations (MIMOs) and zero-resistance states (ZRS) in high-mobility two-dimensional (2D) electron gas (EG)[1–4] has stimulated tremendous experimental[5–14] and theoretical[15–33] interest in radiation-related magnetotransport in 2D electron systems. Since theoretically it has been shown that the ZRS can be the result of the instability induced by absolute negative resistivity,[19] the majority of microscopic models focus mainly on MIMOs in spatially uniform cases and identify the region where a negative dissipative magnetoresistance develops as that of a measured zero resistance. Most of the previous investigations concentrated on the range of low magnetic fields, $\omega_c/\omega \leqslant 1$ (ω_c stands for the cyclotron frequency), subject to a radiation of frequency $\omega/2\pi \leqslant 100$ GHz, where MIMOs show up strongly and Shubnikov–de Haas oscillations (SdHOs) are rarely appreciable. In spite of the fact that both MIMOs and SdHOs are magnetoresistance-related phenomena appearing in overlapping field regimes, little attention was paid to the influence of a microwave radiation on SdHO until a recent experimental finding at higher frequency.[11] Further observations clearly show that the amplitudes of SdHOs are strongly affected by microwave radiations of different frequency in both low ($\omega_c/\omega < 1$) and high ($\omega_c/\omega > 1$) magnetic field ranges.[12–14] Kovalev *et al.*[11] observed a suppression of the SdHOs around a cyclotron resonance of $\omega_c \sim \omega$, induced by a radiation of 285 GHz. Du *et al.*[12] found strong modulations of SdHO in an ultraclean 2D sample subjected to microwaves of 146 GHz, clearly showing, in addition to the first node at $\omega/\omega_c = 1$, higher-order nodes around $\omega/\omega_c = 2$ and 3. Mani[13] reported strong modulation in the amplitude of SdHOs accompanying MIMOs and zero-resistance states excited by 163.5-GHz radiation and a large dropoff of the dissipative resistivity below its dark value at the high ($\omega_c/\omega > 1$) field side when subjected to low-frequency radiation. Very recently, Dorozhkin *et al.*[14] reported both strong suppression of the magnetoresistance caused by radiation below 30 GHz and an interesting modulation of SdHOs in the range $\omega_c/\omega > 1$. They found that SdHOs are generally strongly damped by the radiation, but there is a narrow magnetic field range in between the allowed ranges of inter- and intra-Landau level transitions, where the amplitude of SdHO is insensitive to the microwave irradiation. These observations provide a more complicated and appealing picture of the microwave-related transport phenomena, which must be accounted for in any theoretical model for MIMOs.

We propose that these SdHO modulations come from electron heating induced by microwave radiation. Under microwave illumination, the electron system, which continuously absorbs energy from the radiation field, would certainly be heated. Unfortunately, the electron heating has so far been ignored in most of the theoretical treatments. The electron-acoustic phonon interaction was previously considered to contribute to Landau-level broadening[24] or to act as a damping[31] for the orbit movement, providing a mechanism for the suppression of MIMOs when the lattice temperature increases. Besides, the inelastic electron-phonon scattering also plays another important role to dissipate energy from the electron system to the lattice. The energy absorption rate is indeed small in high-mobility electron systems at low temperatures, as shown in the experiments. This, however, does not imply a negligible electron heating, since the electron energy-dissipation rate is also small because of weak electron-phonon scattering at temperature $T \leqslant 1$ K. To deal with SdHO, which is very sensitive to the smearing of the electron distribution, one has to carefully calculate the electron heating due to microwave irradiation in a uniform model.

On the other hand, microwave irradiation heats the electrons and thus greatly strengthens the thermalizing trend of the system by enhancing the electron-electron scattering rate at this low-temperature regime. This enables us to describe these high-mobility 2D electron systems with a quasiequilibrium distribution in a moving reference frame.

In this paper we pursue a theoretical investigation on MIMOs and SdHOs, taking into account electron heating under microwave irradiation. We generalize the balance equation approach to radiation-induced magnetotransport in high-mobility 2D electron systems. By carefully calculating the electron heating based on the balance of the energy absorption from the radiation field and the energy dissipation to the lattice through electron-phonon interactions in a typical GaAs-based heterosystem and taking into account the electrodynamic effect, we are able not only to reproduce the interesting phenomena of MIMOs, in quantitative agreement with experiments in amplitudes, phases, and radiation dependence of the oscillation, but also to obtain SdHO modulations observed in the experiments.

II. FORMULATION

A. Force- and energy-balance equations

This paper is concerned with the magnetotransport in a microscopically homogeneous 2D system, and refers the measured zero resistance to the macroscopic consequence of the instability due to the occurrence of negative dissipative resistivity.

We consider N_e electrons in a unit area of an infinite quasi-2D system in the x-y plane with a confining potential $V(z)$ in the z direction. These electrons, in addition to interacting with each other, are scattered by random impurities and/or disorders and by phonons in the lattice. Within the magnetic field range relevant to the MIMO phenomenon, the experiments exclude the onset of the quantum Hall effect, thus allowing us to assume that the 2D electrons are in extended states.

To include possible elliptically polarized microwave illumination we assume that a dc electric field $\mathbf{E}_0$ and a high-frequency (HF) ac field of angular frequency ω,

$$\mathbf{E}(t) \equiv \mathbf{E}_s \sin(\omega t) + \mathbf{E}_c \cos(\omega t), \tag{1}$$

are applied inside the 2D system in the x-y plane, together with a magnetic field $\mathbf{B}=(0,0,B)$ along the z direction. The spatial homogeneity of the fields and the parabolic band structure allows to describe the transport of this system in terms of its center-of-mass (c.m.) motion and the relative motion, i.e., the motion of electrons in the reference frame moving with the c.m.[34–36] The c.m. momentum and coordinate of the 2D electron system are defined as $\mathbf{P}\equiv\Sigma_j \mathbf{p}_{j\|}$ and $\mathbf{R}\equiv N_e^{-1}\Sigma_j \mathbf{r}_{j\|}$, with $\mathbf{p}_{j\|}\equiv(p_{jx},p_{jy})$ and $\mathbf{r}_{j\|}\equiv(x_j,y_j)$ being the momentum and coordinate of the jth electron in the 2D plane, respectively, and the relative electron momentum and coordinate are defined as $\mathbf{p}'_{j\|}\equiv\mathbf{p}_{j\|}-\mathbf{P}/N_e$ and $\mathbf{r}'_{j\|}\equiv\mathbf{r}_{j\|}-\mathbf{R}$, respectively. In terms of these variables, the Hamiltonian of the system, H, can be written as the sum of a c.m. part H_{cm} and a relative electron part H_{er} [$\mathbf{A}(\mathbf{r})$ is the vector potential of the $\mathbf{B}$ field],

$$H_{cm} = \frac{1}{2N_e m}(\mathbf{P} - N_e e\mathbf{A}(\mathbf{R}))^2 - N_e e(\mathbf{E}_0 + \mathbf{E}(t))\cdot\mathbf{R}, \tag{2}$$

$$H_{er} = \sum_j \left\{ \frac{1}{2m}[\mathbf{p}'_{j\|} - e\mathbf{A}(\mathbf{r}'_{j\|})]^2 + \frac{p_{jz}^2}{2m_z} + V(z_j) \right\} + \sum_{i<j} V_c(\mathbf{r}'_{i\|} - \mathbf{r}'_{j\|}, z_i, z_j), \tag{3}$$

together with electron-impurity and electron-phonon interactions

$$H_{ei} = \sum_{j,a,\mathbf{q}_\|} u(\mathbf{q}_\|, z_a) e^{i\mathbf{q}_\|\cdot(\mathbf{R}+\mathbf{r}'_{j\|}-\mathbf{r}_{a\|})}, \tag{4}$$

$$H_{ep} = \sum_{j,\mathbf{q}_\|} M(\mathbf{q}_\|, q_z)(b_\mathbf{q} + b_\mathbf{q}^\dagger) e^{i\mathbf{q}_\|\cdot(\mathbf{R}+\mathbf{r}'_{j\|})}. \tag{5}$$

Here m and m_z are, respectively, the electron effective mass parallel and perpendicular to the 2D plane, and V_c stands for the electron-electron Coulomb interaction; $u(\mathbf{q}_\|, z_a)$ is the potential of the ath impurity located at $(\mathbf{r}_{a\|}, z_a)$; $b_\mathbf{q}^\dagger(b_\mathbf{q})$ are the creation (annihilation) operators of the bulk phonon with wave vector $\mathbf{q}=(\mathbf{q}_\|, q_z)$, and $M(\mathbf{q}_\|, q_z)$ is the matrix element of the electron-phonon interaction in the 3D plane-wave representation. Note that the uniform electric field (dc and ac) appears only in H_{cm}, and that H_{er} is just the Hamiltonian of a quasi-2D system subjected to a magnetic field without an electric field. The coupling between the c.m. and the relative electrons appears only in the exponential factor $\exp(i\mathbf{q}_\|\cdot\mathbf{R})$ inside the 2D momentum $\mathbf{q}_\|$ summation in H_{ei} and H_{ep}.[36] The balance equation treatment starts with the Heisenberg operator equation for the rate of change of the c.m. velocity $\dot{\mathbf{V}} = -i[\mathbf{V},H] + \partial\mathbf{V}/\partial t$ with $\mathbf{V}=-i[\mathbf{R},H]$, and that for the rate of change of the relative electron energy $\dot{H}_{er}=-i[H_{er},H]$. Then we proceed with the determination of their statistical averages.

As proposed in Ref. 35, the c.m. coordinate operator $\mathbf{R}$ and velocity operator $\mathbf{V}$ can be treated classically, i.e., as the time-dependent expectation values of the c.m. coordinate and velocity, $\mathbf{R}(t)$ and $\mathbf{V}(t)$, such that $\mathbf{R}(t)-\mathbf{R}(t')=\int_{t'}^{t}\mathbf{V}(s)ds$. We are concerned with the steady transport state under an irradiation of single frequency and focus on the photon-induced dc resistivity and the energy absorption of the HF field. These quantities are directly related to the time-averaged and/or base-frequency oscillating components of the c.m. velocity. Although higher harmonics of the current may affect the dc and lower harmonic terms of the drift velocity by entering the damping force and energy exchange rates in the resulting equations, in an ordinary semiconductor the power of even the third harmonic current is rather weak as compared to the fundamental current. For the HF field intensity in the MIMO experiments, the effect of the higher harmonic current is safely negligible. Hence, it suffices to assume that the c.m. velocity, i.e., the electron drift velocity, consists of a dc part $\mathbf{v}_0$ and a stationary time-dependent part $\mathbf{v}(t)$ of the form

$$\mathbf{V}(t) = \mathbf{v}_0 - \mathbf{v}_1\cos(\omega t) - \mathbf{v}_2\sin(\omega t). \tag{6}$$

With this, the exponential factor in the operator equations can be expanded in terms of Bessel functions $J_n(x)$,

$$e^{i\mathbf{q}_\parallel\cdot\int_{t'}^{t}\mathbf{V}(s)ds}=\sum_{n=-\infty}^{\infty}J_n^2(\xi)e^{i(\mathbf{q}_\parallel\cdot\mathbf{v}_0-n\omega)(t-t')}+\sum_{m\neq 0}e^{im(\omega t-\varphi)}\sum_{n=-\infty}^{\infty}J_n(\xi)J_{n-m}(\xi)e^{i(\mathbf{q}_\parallel\cdot\mathbf{v}_0-n\omega)(t-t')}.$$

Here the argument in the Bessel functions

$$\xi\equiv\frac{1}{\omega}[(\mathbf{q}_\parallel\cdot\mathbf{v}_1)^2+(\mathbf{q}_\parallel\cdot\mathbf{v}_2)^2]^{1/2}, \tag{7}$$

and $\tan\varphi=(\mathbf{q}_\parallel\cdot\mathbf{v}_2)/(\mathbf{q}_\parallel\cdot\mathbf{v}_1)$.

Under the influence of a modest-strength HF electric field the electron system is far from equilibrium. However, the distribution function of relative electrons, which experience no electric field directly, may be close to a quasiequilibrium-type distribution function. For the experimental GaAs-based ultraclean 2D electron systems having a carrier mobility of the order of 2000 m^2/V s, the elastic momentum scattering rate is around $\tau_m^{-1}\sim 10$ mK. In these systems, the thermalization time τ_{th} (i.e., the time for the system to return to its internal equilibrating state when it is deviated from), estimated conservatively using an electron-electron (e-e) interaction-related inelastic scattering time τ_{ee} calculated with an equilibrium distribution function at temperature $T=1$ K, is also around $\tau_{th}^{-1}\sim\tau_{ee}^{-1}\sim 10$ mK. The microwave illumination certainly heats the electrons. Even an electron heating comparable to a temperature rise of a couple of degrees would greatly enhance τ_{ee}^{-1}, such that the thermalization time τ_{th} would become much shorter than the momentum relaxation time τ_m under microwave irradiation.[37] The relative electron systems subject to a modest radiation would rapidly thermalize, and can thus be described reasonably by a Fermi-type distribution function at an average electron temperature T_e in the reference frame moving with the c.m. This allows us to carry out the statistical average of the operator equations for the rates of changes of the c.m. velocity $\mathbf{V}$ and relative electron energy H_{er} to the leading order in H_{ei} and H_{ep} with succinct forms.

For the determination of unknown parameters $\mathbf{v}_0$, $\mathbf{v}_1$, $\mathbf{v}_2$, and T_e, it suffices to know the damping force up to the base frequency oscillating term $\mathbf{F}(t)=\mathbf{F}_0+\mathbf{F}_s\sin(\omega t)+\mathbf{F}_c\cos(\omega t)$, and the energy-related quantities up to the time-averaged terms. We finally obtain the force and energy balance equations,

$$N_e e\mathbf{E}_0+N_e e(\mathbf{v}_0\times\mathbf{B})+\mathbf{F}_0=0, \tag{8}$$

$$\mathbf{v}_1=\frac{e\mathbf{E}_s}{m\omega}+\frac{\mathbf{F}_s}{N_e m\omega}-\frac{e}{m\omega}(\mathbf{v}_2\times\mathbf{B}), \tag{9}$$

$$-\mathbf{v}_2=\frac{e\mathbf{E}_c}{m\omega}+\frac{\mathbf{F}_c}{N_e m\omega}-\frac{e}{m\omega}(\mathbf{v}_1\times\mathbf{B}), \tag{10}$$

$$N_e e\mathbf{E}_0\cdot\mathbf{v}_0+S_p-W=0. \tag{11}$$

Here

$$\mathbf{F}_0=\sum_{\mathbf{q}_\parallel}|U(\mathbf{q}_\parallel)|^2\sum_{n=-\infty}^{\infty}\mathbf{q}_\parallel J_n^2(\xi)\Pi_2(\mathbf{q}_\parallel,\omega_0-n\omega)+\sum_{\mathbf{q}}|M(\mathbf{q})|^2\sum_{n=-\infty}^{\infty}\mathbf{q}_\parallel J_n^2(\xi)\Lambda_2(\mathbf{q},\omega_0+\Omega_{\mathbf{q}}-n\omega) \tag{12}$$

is the time-averaged damping force,

$$S_p=\sum_{\mathbf{q}_\parallel}|U(\mathbf{q}_\parallel)|^2\sum_{n=-\infty}^{\infty}n\omega J_n^2(\xi)\Pi_2(\mathbf{q}_\parallel,\omega_0-n\omega)+\sum_{\mathbf{q}}|M(\mathbf{q})|^2\sum_{n=-\infty}^{\infty}n\omega J_n^2(\xi)\Lambda_2(\mathbf{q},\omega_0+\Omega_{\mathbf{q}}-n\omega) \tag{13}$$

is the time-averaged rate of the electron energy absorption from the HF field, and

$$W=\sum_{\mathbf{q}}|M(\mathbf{q})|^2\sum_{n=-\infty}^{\infty}\Omega_{\mathbf{q}}J_n^2(\xi)\Lambda_2(\mathbf{q},\omega_0+\Omega_{\mathbf{q}}-n\omega) \tag{14}$$

is the time-averaged rate of the electron energy dissipation to the lattice due to electron-phonon scatterings. The oscillating frictional force amplitudes $\mathbf{F}_s\equiv\mathbf{F}_{22}-\mathbf{F}_{11}$ and $\mathbf{F}_c\equiv\mathbf{F}_{21}+\mathbf{F}_{12}$ are given by $(\mu=1,2)$

$$\mathbf{F}_{1\mu}=-\sum_{\mathbf{q}_\parallel}\mathbf{q}_\parallel\eta_\mu|U(\mathbf{q}_\parallel)|^2\sum_{n=-\infty}^{\infty}[J_n^2(\xi)]'\Pi_1(\mathbf{q}_\parallel,\omega_0-n\omega)-\sum_{\mathbf{q}}\mathbf{q}_\parallel\eta_\mu|M(\mathbf{q})|^2\sum_{n=-\infty}^{\infty}[J_n^2(\xi)]'\Lambda_1(\mathbf{q},\omega_0+\Omega_{\mathbf{q}}-n\omega), \tag{15}$$

$$\mathbf{F}_{2\mu}=\sum_{\mathbf{q}_\parallel}\mathbf{q}_\parallel\frac{\eta_\mu}{\xi}|U(\mathbf{q}_\parallel)|^2\sum_{n=-\infty}^{\infty}2nJ_n^2(\xi)\Pi_2(\mathbf{q}_\parallel,\omega_0-n\omega)+\sum_{\mathbf{q}}\mathbf{q}_\parallel\frac{\eta_\mu}{\xi}|M(\mathbf{q})|^2\sum_{n=-\infty}^{\infty}2nJ_n^2(\xi)\Lambda_2(\mathbf{q},\omega_0+\Omega_{\mathbf{q}}-n\omega). \tag{16}$$

In these expressions, $\eta_\mu\equiv\mathbf{q}_\parallel\cdot\mathbf{v}_\mu/\omega\xi$; $\omega_0\equiv\mathbf{q}_\parallel\cdot\mathbf{v}_0$; $U(\mathbf{q}_\parallel)$ and $M(\mathbf{q})$ are the effective impurity and phonon scattering potentials (including effects of the spatial distribution of impurities and the form factor of quasi-2D electrons).[36] $\Pi_2(\mathbf{q}_\parallel,\Omega)$ and $\Lambda_2(\mathbf{q},\Omega)=2\Pi_2(\mathbf{q}_\parallel,\Omega)[n(\Omega_{\mathbf{q}}/T)-n(\Omega/T_e)]$ [with $n(x)\equiv 1/(e^x-1)$] are the imaginary parts of the electron density correlation function and electron-phonon correlation function in the presence of the magnetic field. $\Pi_1(\mathbf{q}_\parallel,\Omega)$ and $\Lambda_1(\mathbf{q},\Omega)$ are the real parts of these two correlation functions.

Effects of microwave radiation on electron transport first come from the HF field-induced c.m. motion (electron drift motion) and the related change of the electron distribution. In addition to this, the HF field also enters via the argument ξ of the Bessel functions in $\mathbf{F}_0$, $\mathbf{F}_{\mu\nu}$, W, and S_p. Compared with that without a HF field, we see that in an electron gas having an impurity and/or phonon scattering (otherwise ho-

mogeneous), a HF field of frequency ω opens additional channels for electron transition: an electron in a state can absorb or emit one or several photons of frequency ω and scattered to a different state with the help of impurities and/or phonons. The sum over $|n| \geqslant 1$ represents contributions of real single and multiple photon participating processes. The role of these processes is twofold. On the one hand, they contribute additional damping force to the moving electrons, giving rise directly to photoresistance, and at the same time, transfer energy from the HF field to the electron system, resulting in electron heating, i.e., another change (smearing) in the electron distribution.[38] Furthermore, the radiation field, showing up in the term with $J_0(\xi)$ in $\mathbf{F}_0$, $\mathbf{F}_{\mu\nu}$ and W, gives rise to another effective change of damping forces and energy-loss rate, without emission or absorption of real photons. This virtual photon process also contributes to photoresistance.[39] All these effects are carried by parameters $\mathbf{v}_0$, $\mathbf{v}_1$, $\mathbf{v}_2$ and T_e. Equations (8)–(11) form a closed set of equations for the determination of these parameters when $\mathbf{E}_0$, $\mathbf{E}_c$, and $\mathbf{E}_s$ are given in a 2D system subjected to a magnetic field B at temperature T.

B. Longitudinal and transverse resistivities

The nonlinear resistivity in the presence of a high-frequency field is easily obtained from Eq. (8). Taking $\mathbf{v}_0$ to be in the x direction, $\mathbf{v}_0=(v_{0x},0,0)$, we immediately get the transverse and longitudinal resistivities,

$$R_{xy} \equiv \frac{E_{0y}}{N_e e v_{0x}} = \frac{B}{N_e e}, \tag{17}$$

$$R_{xx} \equiv \frac{E_{0x}}{N_e e v_{0x}} = -\frac{F_0}{N_e^2 e^2 v_{0x}}. \tag{18}$$

The linear magnetoresistivity is the weak dc current limit ($v_{0x} \to 0$),

$$R_{xx} = -\sum_{\mathbf{q}_\parallel} q_x^2 \frac{|U(\mathbf{q}_\parallel)|^2}{N_e^2 e^2} \sum_{n=-\infty}^{\infty} J_n^2(\xi) \left.\frac{\partial \Pi_2}{\partial \Omega}\right|_{\Omega=n\omega} - \sum_{\mathbf{q}} q_x^2 \frac{|M(\mathbf{q})|^2}{N_e^2 e^2} \sum_{n=-\infty}^{\infty} J_n^2(\xi) \left.\frac{\partial \Lambda_2}{\partial \Omega}\right|_{\Omega=\Omega_{\mathbf{q}}+n\omega}. \tag{19}$$

Note that although according to Eqs. (12), (18), and (19), the longitudinal magnetoresistivity R_{xx} can be formally written as the sum of contributions from various individual scattering mechanisms, all the scattering mechanisms have to be taken into account simultaneously in solving the momentum- and energy-balance equations (9)–(11), for $\mathbf{v}_1$, $\mathbf{v}_2$, and T_e, which enter the Bessel functions and other parts in the expression of R_{xx}.

C. Landau-level broadening

In the present model the effects of interparticle Coulomb screening are included in the electron complex density correlation function $\Pi(\mathbf{q}_\parallel,\Omega)=\Pi_1(\mathbf{q}_\parallel,\Omega)+i\Pi_2(\mathbf{q}_\parallel,\Omega)$, which, in the random-phase approximation, can be expressed as

$$\Pi(\mathbf{q}_\parallel,\Omega) = \frac{\Pi_0(\mathbf{q}_\parallel,\Omega)}{\epsilon(\mathbf{q}_\parallel,\Omega)}, \tag{20}$$

where

$$\epsilon(\mathbf{q}_\parallel,\Omega) \equiv 1 - V(q_\parallel)\Pi_0(\mathbf{q}_\parallel,\Omega) \tag{21}$$

is the complex dynamical dielectric function,

$$V(q_\parallel) = \frac{e^2}{2\epsilon_0 \kappa q_\parallel} H(q_\parallel) \tag{22}$$

is the effective Coulomb potential with κ the dielectric constant of the material and $H(q_\parallel)$ is a 2D wave-function-related overlapping integration,[36] and $\Pi_0(\mathbf{q}_\parallel,\Omega)=\Pi_{01}(\mathbf{q}_\parallel,\Omega)+i\Pi_{02}(\mathbf{q}_\parallel,\Omega)$ is the complex density correlation function of the independent electron system in the presence of the magnetic field. With this dynamically screened density correlation function the collective plasma modes of the 2DES are incorporated. Disregarding these collective modes, one can just use a static screening of $\epsilon(\mathbf{q}_\parallel,0)$ instead.

The $\Pi_{02}(\mathbf{q}_\parallel,\Omega)$ function of a 2D system in a magnetic field can be written in terms of the Landau representation[34]

$$\Pi_{02}(\mathbf{q}_\parallel,\Omega) = \frac{1}{2\pi l_B^2} \sum_{n,n'} C_{n,n'}(l_B^2 q_\parallel^2/2)\Pi_2(n,n',\Omega), \tag{23}$$

$$\Pi_2(n,n',\Omega) = -\frac{2}{\pi}\int d\varepsilon [f(\varepsilon) - f(\varepsilon+\Omega)] \times \mathrm{Im}\, G_n(\varepsilon+\Omega)\mathrm{Im}\, G_{n'}(\varepsilon), \tag{24}$$

where $l_B=\sqrt{1/|eB|}$ is the magnetic length,

$$C_{n,n+l}(Y) \equiv n![(n+l)!]^{-1} Y^l e^{-Y} [L_n^l(Y)]^2, \tag{25}$$

with $L_n^l(Y)$ the associate Laguerre polynomial, $f(\varepsilon)=\{\exp[(\varepsilon-\mu)/T_e]+1\}^{-1}$ the Fermi distribution function, and $\mathrm{Im}\, G_n(\varepsilon)$ is the imaginary part of the electron Green's function, or the density of states (DOS), of the Landau level n. The real part function $\Pi_{01}(\mathbf{q}_\parallel,\Omega)$ and corresponding $\Lambda_{01}(\mathbf{q}_\parallel,\Omega)$ function can be derived from their imaginary parts via the Kramers-Kronig relation.

In principle, to obtain the Green's function $\mathrm{Im}\, G_n(\varepsilon)$, a self-consistent calculation has to be carried out from the Dyson equation for the self-energy with all the impurity, phonon, and e-e scatterings included. The resultant G_n is generally a complicated function of the magnetic field, temperature, and Landau-level index n, also dependent on different kinds of scatterings. Such a calculation is beyond the scope of the present study. In this paper we model the DOS function with a Gaussian-type form (ε_n is the energy of the nth Landau level)[40,41]

$$\mathrm{Im}\, G_n(\varepsilon) = -\frac{\sqrt{2\pi}}{\Gamma}\exp\left[-\frac{2(\varepsilon-\varepsilon_n)^2}{\Gamma^2}\right], \tag{26}$$

with a broadening width given by

$$\Gamma = \left(\frac{8e\omega_c\alpha}{\pi m\mu_0}\right)^{1/2}, \tag{27}$$

where μ_0 is the linear mobility in the absence of the magnetic field and α is a semiempirical parameter to take into account the difference of the transport scattering time τ_m determining the mobility μ_0, from the single particle lifetime τ_s related to Landau-level broadening. The latter depends on elastic scatterings of different types and their relative strengths, as well as contributions of electron-phonon and electron-electron scatterings. α will serve as the only adjustable parameter in the present investigation. Unlike the semielliptic function, which can model only a separated Landau-level case, a Gaussian-type broadening function can reasonably cover both the separated-level and overlapping-level regimes.

D. Effect of radiative decay

The HF electric field $\mathbf{E}(t)$ appearing in Eqs. (8) and (9) is the total (external and induced) field actually acting on the 2D electrons. Experiments are always performed under the condition of giving external radiation. In this paper we assume that the electromagnetic wave is incident perpendicularly (along the z axis) upon 2DEG from the vacuum with an incident electric field of

$$\mathbf{E}_{\mathrm{i}}(t) = \mathbf{E}_{\mathrm{i}s}\sin(\omega t) + \mathbf{E}_{\mathrm{i}c}\cos(\omega t) \tag{28}$$

at plane $z=0$. The relation between $\mathbf{E}(t)$ and $\mathbf{E}_{\mathrm{i}}(t)$ is easily obtained by solving the Maxwell equations connecting both sides of the 2DEG, which is carrying a sheet current density of $N_{\mathrm{e}}e\mathbf{v}(t)$. If the 2DEG locates under the surface plane at $z=0$ of a thick (treated as semi-infinite) semiconductor substrate having a refraction index n_s, we have[42,43]

$$\mathbf{E}(t) = \frac{N_{\mathrm{e}}e\mathbf{v}(t)}{(1+n_s)\epsilon_0 c} + \frac{2}{1+n_s}\mathbf{E}_{\mathrm{i}}(t). \tag{29}$$

If the 2DEG is contained in a thin sample suspended in vacuum at the plane $z=0$, then

$$\mathbf{E}(t) = \frac{N_{\mathrm{e}}e\mathbf{v}(t)}{2\epsilon_0 c} + \mathbf{E}_{\mathrm{i}}(t). \tag{30}$$

In the numerical calculation of this paper we consider the latter case and use Eq. (30) for the total self-consistent field $\mathbf{E}(t)$ in Eqs. (9) and (10). This electrodynamic effect,[42,43] recently referred to as radiative decay,[27] gives rise to an additional damping in the 2DEG response to a given incident HF field. The induced damping turns out to be much stronger than the intrinsic damping due to scattering-related forces $\mathbf{F}_s$ and $\mathbf{F}_c$ for the experimental high-mobility systems at low temperatures. For almost all the cases pertinent to MIMO experiments we can neglect the forces $\mathbf{F}_s$ and $\mathbf{F}_c$ completely in solving $\mathbf{v}_1 \equiv (v_{1x}, v_{1y})$ and $\mathbf{v}_2 \equiv (v_{2x}, v_{2y})$ from Eqs. (9) and (10) for given incident fields $\mathbf{E}_{\mathrm{i}s}$ and $\mathbf{E}_{\mathrm{i}c}$, and obtain explicitly

$$v_{1x} = (a\chi_{sx} + b\chi_{sy})/\Delta,$$

$$v_{1y} = (a\chi_{sy} - b\chi_{sx})/\Delta,$$

$$v_{2x} = (-a\chi_{cx} - b\chi_{cy})/\Delta,$$

$$v_{2y} = (-a\chi_{cy} + b\chi_{cx})/\Delta, \tag{31}$$

with $\Delta = (1-\delta_\omega^2+\gamma_\omega^2)^2 + (2\gamma_\omega\delta_\omega)^2$, and

$$\chi_{sx} = \nu_{sx} - \delta_\omega\nu_{cy} + \gamma_\omega\nu_{cx},$$

$$\chi_{sy} = \nu_{sy} + \delta_\omega\nu_{cx} + \gamma_\omega\nu_{cy},$$

$$\chi_{cx} = \nu_{cx} + \delta_\omega\nu_{sy} - \gamma_\omega\nu_{sx},$$

$$\chi_{cy} = \nu_{cy} - \delta_\omega\nu_{sx} + \gamma_\omega\nu_{sy}. \tag{32}$$

Here

$$\nu_\eta \equiv -\frac{eE_{\mathrm{i}\eta}}{m\omega}(\eta = sx, sy, cx, cy), \tag{33}$$

$\delta_\omega \equiv \omega_c/\omega$ and $\gamma_\omega \equiv \gamma/\omega$ with

$$\gamma = \frac{N_{\mathrm{e}}e^2}{2m\epsilon_0 c}. \tag{34}$$

With these $\mathbf{v}_1$ and $\mathbf{v}_2$, the argument ξ entering the Bessel functions is obtained. All the transport quantities, such as S_{p}, W, and R_{xx}, can be calculated directly with the electron temperature T_{e} determined from the energy balance equation (11).

III. NUMERICAL RESULTS FOR GaAs-BASED SYSTEMS

As in the experiments, we focus our attention on high-mobility 2DEGs formed by GaAs/AlGaAs heterojunctions. For these systems at temperature $T \leqslant 1$ K, the dominant contributions to the energy absorption S_{p} and photoresistivity $R_{xx}-R_{xx}(0)$ come from the impurity-assisted photon-absorption and emission process. At different magnetic field strengths, this process is associated with electron transitions between either inter-Landau level states or intra-Landau-level states. According to (26), the width of each Landau level is about 2Γ. The condition for inter-Landau level transition with an impurity-assisted single-photon process[44] is $\omega > \omega_c - 2\Gamma$ or $\omega_c/\omega < a_{\mathrm{inter}} = (\beta + \sqrt{\beta^2+4})^2/4$, and that for the impurity-assisted intra-Landau level transition is $\omega < 2\Gamma$ or $\omega_c/\omega > a_{\mathrm{intra}} = \beta^{-2}$, where $\beta = (32e\alpha/\pi m\mu_0\omega)^{1/2}$. However, since the DOS of each Landau level is assumed to be Gaussian rather than a clear cutoff function, and the multiphoton processes also play roles, the transition boundaries between different regimes may be somewhat smeared.

As indicated by experiments,[45] although long-range scattering due to remote donors always exists in the 2D heterostructures, in ultraclean GaAs-based 2D samples having mobilities of the order of 10^3 m^2/V s, the remote donor scattering is responsible for merely $\sim$10% or less of the total momentum scattering rate. The dominant contribution to the momentum scattering rate comes from short-range scatterers such as residual impurities or defects in the background. Furthermore, even with the same momentum scattering rate, the remote impurity scattering is much less efficient in contrib-

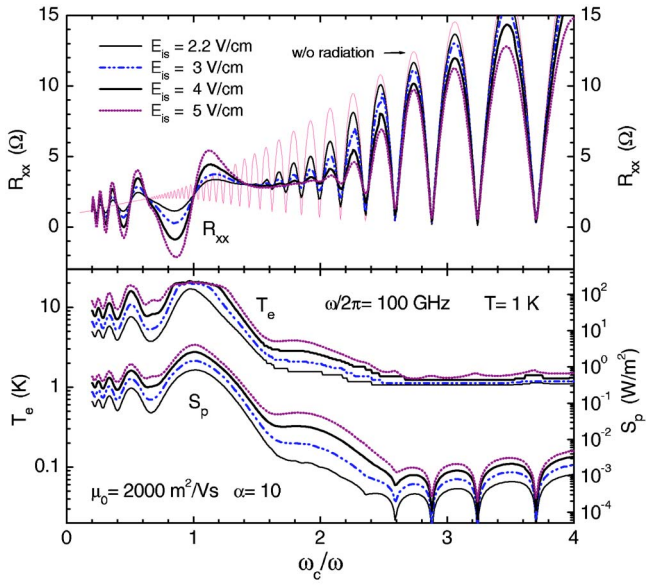

FIG. 1. (Color online) The magnetoresistivity R_{xx}, electron temperature T_e, and energy absorption rate S_p of a GaAs-based 2DEG with $\mu_0=2000$ m^2/V s and $\alpha=10$, subjected to 100-GHz linearly x-polarized incident HF fields $E_{is}\sin(\omega t)$ of four different strengths. The lattice temperature is $T=1$ K.

uting to microwave-induced magnetoresistance oscillations than short-ranged background impurities or defects.[46] Therefore, in the numerical calculations in this paper we assume that the elastic scatterings are due to short-range impurities randomly distributed throughout the GaAs region. The impurity densities are determined by the requirement that electron total linear mobility at zero magnetic field equals the given value at lattice temperature T. Possibly, long-range remote donor scattering may give rise to important contributions to Landau-level broadening. This effect, together with the role of electron-phonon and electron-electron scatterings, is included in the semiempirical parameter α in expression (27).

In order to obtain the energy dissipation rate from the electron system to the lattice, W, we take into account scatterings from bulk longitudinal acoustic (LA) and transverse acoustic (TA) phonons (via the deformation potential and piezoelectric couplings), as well as from longitudinal optical (LO) phonons (via the Fröhlich coupling) in the GaAs-based system. The relevant matrix elements are well known.[36] The material and coupling parameters for the system are taken to be widely accepted values in bulk GaAs: electron effective mass $m=0.068m_e$ (m_e is the free-electron mass), transverse sound speed $v_{st}=2.48\times10^3$ m/s, longitudinal sound speed $v_{sl}=5.29\times10^3$ m/s, acoustic deformation potential $\Xi=8.5$ eV, piezoelectric constant $e_{14}=1.41\times10^9$ V/m, dielectric constant $\kappa=12.9$, and material mass density $d=5.31$ g/cm^3.

A. 100 GHz

Figure 1 shows the calculated energy absorption rate S_p, the electron temperature T_e, and the longitudinal magnetoresistivity R_{xx} as functions of ω_c/ω for a 2D system having an electron density of $N_e=3.0\times10^{15}$ m^{-2}, a linear mobility of $\mu_0=2000$ m^2/V s, and a broadening parameter of $\alpha=10$, subject to linearly x-direction polarized incident microwave radiations of frequency $\omega/2\pi=100$ GHz having four different amplitudes $E_{is}=2.2$, 3, 4, and 5 V/cm at a lattice temperature of $T=1$ K. The energy absorption rate S_p exhibits a broad main peak at cyclotron resonance $\omega_c/\omega=1$ and secondary peaks at harmonics $\omega_c/\omega=1/2,1/3,1/4$. The electron heating has a similar feature: T_e exhibits peaks around $\omega_c/\omega=1,1/2,1/3,1/4$. For this GaAs system, $\beta=0.65$, $a_{inter}=1.6$, and $a_{intra}=4.7$. We can see that, at lower magnetic fields, especially $\omega_c/\omega<1.4$, the system absorbs enough energy from the radiation field via inter-Landau level transitions and T_e is significantly higher than T, with the maximum as high as 21 K around $\omega_c/\omega=1$. With increasing strength of the magnetic field the inter-Landau level transition weakens (the impurity-assisted single-photon process is mainly allowed when $\omega_c/\omega<a_{inter}=1.6$) and the absorbed energy decreases rapidly. Within the range $2<\omega_c/\omega<4$, before intra-Landau level transitions can take place, S_p is two orders of magnitude smaller than that in the low magnetic field range. Correspondingly, the electron temperature T_e is only slightly higher than the lattice temperature T. The magnetoresistivity R_{xx} shown in the upper part of Fig. 1 exhibits interesting features. MIMOs (with fixed points rather than extrema at $\omega_c/\omega=1,1/2,1/3,1/4$) clearly appear at lower magnetic fields, which are insensitive to the electron heating even at T_e of the order of 20 K. SdHOs appearing in the higher magnetic field side, however, are damped due to the rise of the electron temperature $T_e>1$ K as compared with that without radiation. With an increase in the microwave amplitude from $E_{is}=2.2$ to 5 V/cm, MIMOs become much stronger and SdHOs are further damped. But the radiation-induced SdHO damping is always relatively smaller within $2.4<\omega_c/\omega<4$ between allowed ranges of inter- and intra-Landau level transitions.

It is worth noting that the predicted MIMOs here exhibit much improved agreement with experiments over previous theoretical models. The maxima of R_{xx} oscillation locate at $\omega/\omega_c=j-\delta_-$ and minima at $\omega/\omega_c=j+\delta_+$, with $\delta_\pm\sim0.23-0.25$ for $j=2,3,4\ldots$ and $\delta_\pm\sim0.16-0.20$ (depending on microwave strength) for $j=1$ (see Fig. 2). These phase details, as well as the absolute (rather than reduced) magnitudes of the oscillation amplitudes and the required incident microwave strengths to induce oscillations, are in good quantitative agreement with experiments.[3–7]

The MIMOs depend on the polarization of the incident microwave field with respect to the dc field $\mathbf{E}_0$. Physically this is clear in the present model since it is through the c.m. motion that a HF field affects the photoresistivity of the 2D electron system. Under the influence of a magnetic field perpendicular to the plane, the c.m. performs a cyclic motion of frequency ω_c in the 2D plane. A perpendicularly incident, circularly polarized microwave would accelerate or decelerate this cyclic motion depending on the HF electric field circling with or against it. Thus, at fixed incident power, a left-polarized microwave would yield a much stronger effect on the R_{xx} oscillation than a right-polarized one, and this effect is apparently strongest in the vicinity of cylcotron resonance $\omega_c/\omega=1$. The difference between the x-direction

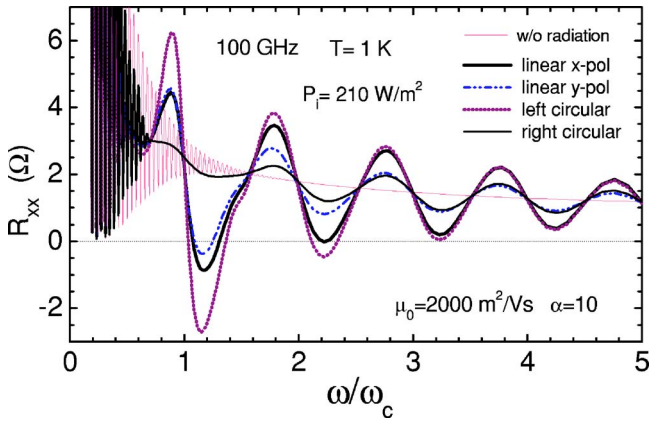

FIG. 2. (Color online) The magnetoresistivity R_{xx} vs ω/ω_c for the same system as described in Fig. 1, subjected to 100-GHz HF radiations of fixed incident power of $P_i=210$ W/m^2 but for four different polarizations.

linearly polarized wave and the y-direction linearly polarized wave, however, comes mainly from the the different angle of radiation-induced c.m. motion with respect to the dc current, and thus not so sensitive to that of the ω_c/ω range. In Fig. 2 we plot the calculated R_{xx} vs ω/ω_c for the same system as described in Fig. 1, subject to a 100-GHz microwave radiation having a fixed incident power of $P_i=210$ W/m^2 (equivalent to an incident amplitude $E_{is}=4$ V/cm of linear polarization) but four different polarizations: linear x polarizaton, linear y polarization, left circular polarization, and right circular polarization. Their difference is clearly seen.

B. 50 GHz and lower frequency

Figure 3 shows the energy absorption rate S_p, the electron temperature T_e, and the longitudinal magnetoresistivity R_{xx} as functions of ω_c/ω for a 2D system having an electron density of $N_e=3.0\times10^{15}$ m^{-2}, a linear mobility of $\mu_0=2500$ m^2/V s, and a broadening parameter of $\alpha=12.5$, subject to linearly x-direction polarized incident microwave radiations of frequency $\omega/2\pi=50$ GHz having four different amplitudes $E_{is}=0.8$, 1.2, 2.0, and 3.5 V/cm at a lattice temperature of $T=1$ K. For this GaAs system at 50 GHz, $a_{\text{inter}}=1.9$ and $a_{\text{intra}}=2.4$. The intra-Landau level single-photon transitions are allowed when $\omega_c/\omega>2.4$, yielding, at the high ω_c/ω side, an absorption rate S_p somewhat larger, an electron temperature T_e somewhat higher and a SdHO damping stronger, than those in the 100-GHz case (Fig. 1). On the other hand, at equivalent HF field strength the multiphoton processes are more important at lower frequency. This helps to enhance the absorption S_p in the range $1.9<\omega_c/\omega<2.4$, where the single-photon process is forbidden and to increase the two-photon resonance in S_p and T_e around $\omega/\omega_c=1.5$, 2.5, and 3.5 (see S_p and T_e curves corresponding to $E_{is}=3.5$ V/cm in Fig. 3). The effect of the two-photon process can also be seen clearly in the R_{xx}-vs-ω/ω_c curves as shown in Fig. 4, where the R_{xx} curve of $E_{is}=3.5$ V/cm V/cm exhibits its obvious shoulders around $\omega/\omega_c=1.5$, 2.5, and 3.5, and descends down around $\omega/\omega_c=0.6$. This kind of two-photon process was clearly seen in the experiments.[4,9]

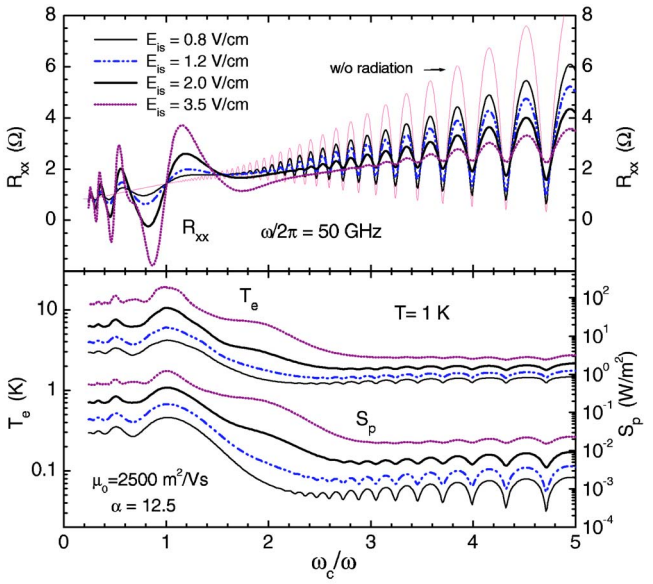

FIG. 3. (Color online) The magnetoresistivity R_{xx}, electron temperature T_e, and energy absorption rate S_p of a GaAs-based 2DEG with $\mu_0=2500$ m^2/V s and $\alpha=12.5$, subjected to 50 GHz linearly x-polarized incident HF fields $E_{is}\sin(\omega t)$ of four different strengths. The lattice temperature is $T=1$ K.

At even lower frequency, such as 30 and 20 GHz, the ranges for intra-Landau level and inter-Landau level single-photon transitions overlap. The enhanced effect of the virtual photon process, together with enhanced multiphoton-assisted electron transition, pushes the resistivity R_{xx} remarkably down below the average of its oscillatory curve without radiation, resulting in a strong suppression of dissipative magnetoresistance across a wide magnetic field rangeas shown in Fig. 5, in agreement with experimental observations.[13,14]

C. 150 and 280 GHz

The radiation-induced SdHO modulation can be seen clearly in the low magnetic field region $\omega/\omega_c>1$ with higher radiation frequency. Figure 6 shows the calculated electron temperature T_e and magnetoresistivity R_{xx} as functions of

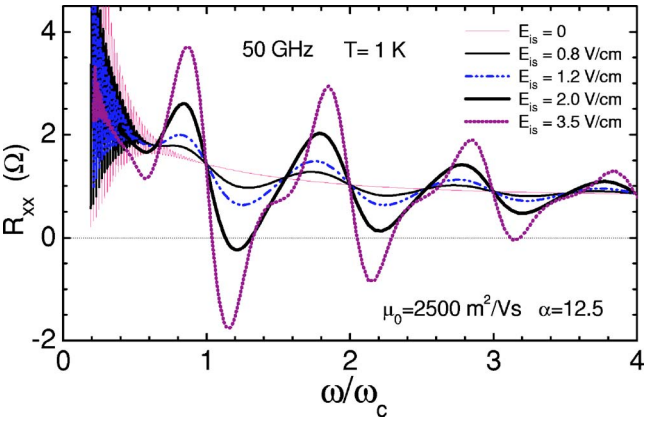

FIG. 4. (Color online) The magnetoresistivity R_{xx} vs ω/ω_c for the same system as described in Fig. 3, subjected to 50-GHz linearly x-polarized incident HF fields of four different strengths.

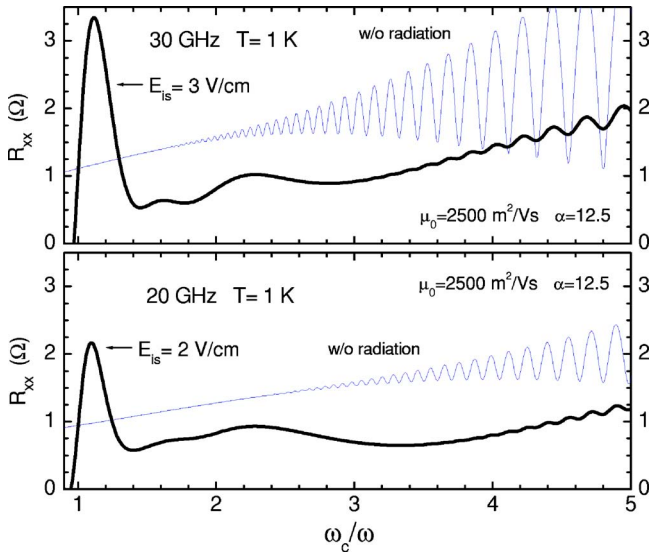

FIG. 5. (Color online) The magnetoresistivity R_{xx} vs ω_c/ω for the same system as described in Fig. 3, subjected to two incident microwave fields: frequency $\omega/2\pi=30$ GHz, amplitude $E_{is}=3$ V/cm (upper figure) and frequency $\omega/2\pi=20$ GHz, amplitude $E_{is}=2$ V/cm (lower figure).

ω/ω_c for a 2D system of electron density $N_e=3.0\times10^{15}$ m^{-2}, linear mobility $\mu_0=2000$ m^2/V s, and $\alpha=3$, subject to a 150-GHz microwave radiation of three different amplitudes $E_{is}=0.1$, 0.6, and 2 V/cm at a lattice temperature of $T=0.5$ K. Low-power microwave illumination ($E_{is}=0.1$ V/cm) already yields sufficient T_e oscillation with maxima at $\omega/\omega_c=1,2,3,4$, giving rise to clear SdHO modulations having nodes at T_e maxima. At higher microwave power ($E_{is}=0.6$ V/cm) when the MIMO shows up, the T_e maxima gets higher, suppressing the SdHO in the vicinities of $\omega/\omega_c=1,2,3,4$, but a strong amplitude modulation of SdHOs is still seen. In the case of $E_{is}=2$ V/cm, R_{xx} shows a strong MIMO and the electron temperature further grows so that most of the SdHOs almost disappear in the range of $\omega/\omega_c>2$. Note that the small T_e peaks at $\omega/\omega_c=1.5$ and 2.5 are due to the absorption rate S_p maxima induced by two-photon processes, which give rise to additional nodes in the SdHOs.

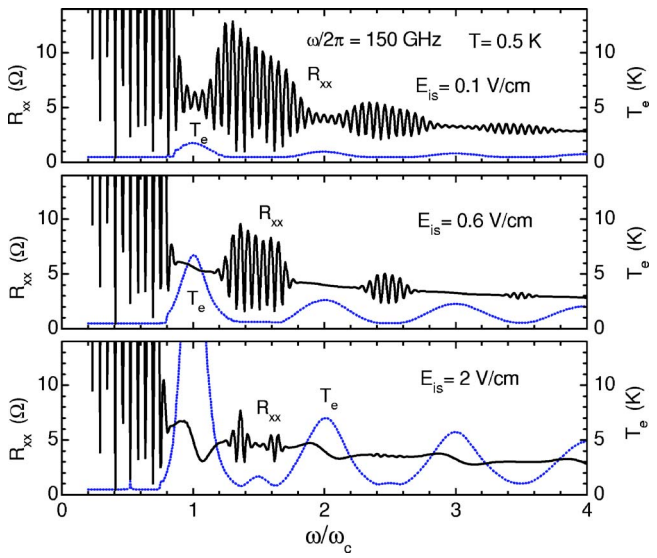

FIG. 6. (Color online) The magnetoresistivity R_{xx} and electron temperature T_e of a GaAs-based 2DEG with $N_e=3.0\times10^{15}$ m^{-2}, $\mu_0=2000$ m^2/V s, and $\alpha=3$, subjected to 150-GHz linearly x-polarized incident HF fields $E_{is}\sin(\omega t)$ of three different strengths $E_{is}=0.1$, 0.6, and 2 V/cm at $T=0.5$ K.

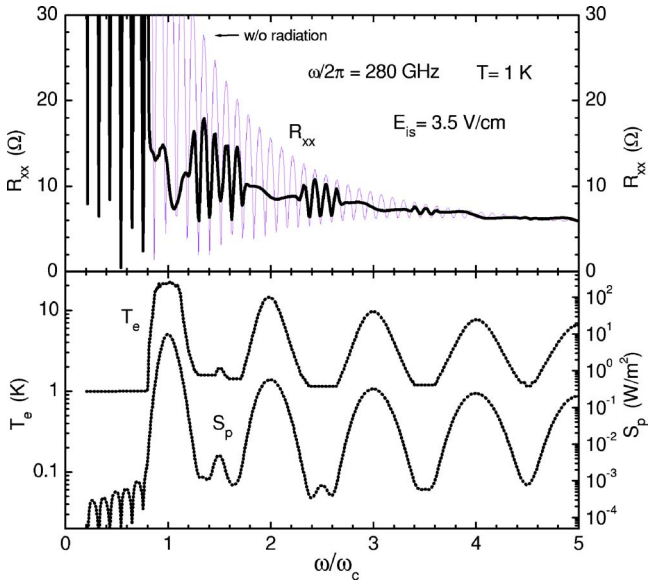

FIG. 7. (Color online) The magnetoresistivity R_{xx}, electron temperature T_e, and energy absorption rate S_p of a GaAs-based 2DEG with $\mu_0=1000$ m^2/V s and $\alpha=2$, subjected to a linearly x-polarized incident HF field of frequency 280 GHz and amplitude $E_{is}=3.5$ V/cm at $T=1$ K.

Another example of the SdHO modulation appearing simultaneously with MIMO is plotted in Fig. 7, where the energy absorption rate S_p, the electron temperature T_e, and the magnetoresistivity R_{xx} are shown as functions of ω/ω_c for a 2D system having an electron density of $N_e=3.0\times10^{15}$ m^{-2}, a linear mobility of $\mu_0=1000$ m^2/V s, and a broadening parameter of $\alpha=2$, subject to linearly x-direction polarized incident microwave radiations of frequency $\omega/2\pi=280$ GHz and amplitude $E_{is}=3.5$ V/cm. The energy absorption rate S_p has broad large peaks at $\omega/\omega_c=1,2,3,4,5$ (due to a single-photon resonant process) and small peaks at $\omega/\omega_c=1.5,2.5$ (due to a two-photon resonant process), giving rise to the oscillation of the electron temperature T_e. One can clearly see the peaks of the electron temperature T_e and the nodes of SdHO modulation at $\omega/\omega_c=1$, 2, 3, 4, and 5, together with MIMOs. These are in agreement with the experimental observation reported in Ref. 11.

D. Discussion

Note that in GaAs-based systems at a temperature of around $T\sim1$ K, LA phonons generally give a larger contribution to the electron energy dissipation W than that from TA phonons, and LO phonons are usually frozen. However, in the case of high radiation power or in the vicinity of $\omega\sim\omega_c$, where the resonantly absorbed energy can be relatively large and the electron temperature can rise up above 20 K, a

weak emission of LO phonons takes place. Although at this temperature the number of excited LO phonons is still very small and their contribution to momentum relaxation (resistivity) is negligible in comparison with acoustic phonons, they can already provide an efficient energy dissipation because each excited LO phonon contributes a huge energy transfer of $\Omega_{\mathrm{LO}} \sim 400$ K. With a continuing rise of electron temperature the LO-phonon contribution increases rapidly. This effectively prevents the electron temperature from going much higher than 20 K, such that the T_e-vs-ω_c/ω curve of large incident microwave power in Fig. 1 exhibits a flat top around $\omega_c/\omega=1$.

In this paper, we did not consider the role of surface or interface phonons in the GaAs heterostructure. Depending on sample geometry, the surface phonons may be important in dissipating electron energy, thus decreasing the electron temperature.

ACKNOWLEDGMENTS

We thank Dr. V. I. Ryzhii, Dr. R. G. Mani, and Dr. R. R. Du for helpful discussions. This work was supported by Projects of the National Science Foundation of China, the Special Funds for Major State Basic Research Project, and the Shanghai Municipal Commission of Science and Technology.

[1] M. A. Zudov, R. R. Du, J. A. Simmons, and J. R. Reno, Phys. Rev. B **64**, 201311(R) (2001).
[2] P. D. Ye, L. W. Engel, D. C. Tsui, J. A. Simmons, J. R. Wendt, G. A. Vawter, and J. L. Reno, Appl. Phys. Lett. **79**, 2193 (2001).
[3] R. G. Mani, J. H. Smet, K. von Klitzing, V. Narayanamurti, W. B. Johnson, and V. Umansky, Nature (London) **420**, 646 (2002).
[4] M. A. Zudov, R. R. Du, L. N. Pfeiffer, and K. W. West, Phys. Rev. Lett. **90**, 046807 (2003).
[5] C. L. Yang, M. A. Zudov, T. A. Knuuttila, R. R. Du, L. N. Pfeiffer, and K. W. West, Phys. Rev. Lett. **91**, 096803 (2003).
[6] S. I. Dorozhkin, JETP Lett. **77**, 577 (2003).
[7] R. G. Mani, J. H. Smet, K. von Klitzing, V. Narayanamurti, W. B. Johnson, and V. Umansky, Phys. Rev. Lett. **92**, 146801 (2004).
[8] R. L. Willett, L. N. Pfeiffer, and K. W. West, Phys. Rev. Lett. **93**, 026804 (2004).
[9] M. A. Zudov, Phys. Rev. B **69**, 041304(R) (2004).
[10] S. A. Studenikin, M. Potenski, A. Sachrajda, M. Hilke, L. N. Pfeiffer, and K. W. West, IEEE Trans. Nanotechnol. **4**, 124 (2005); cond-mat/0411338 (unpublished).
[11] A. E. Kovalev, S. A. Zvyagin, C. R. Bowers, J. L. Reno, and J. A. Simmons, Solid State Commun. **130**, 379 (2004).
[12] R. R. Du, M. A. Zudov, C. L. Yang, Z. Q. Yuan, L. N. Pfeiffer, and K. W. West, Int. J. Mod. Phys. B **18**, 3462 (2004).
[13] R. G. Mani, Physica E (Amsterdam) **22**, 1 (2004); **25**, 189 (2004); Appl. Phys. Lett. **85**, 4962 (2004).
[14] S. I. Dorozhkin, J. H. Smet, V. Umansky, and K. von Klitzing, cond-mat/0409228 (unpublished).
[15] V. I. Ryzhii, Sov. Phys. Solid State **11**, 2087 (1970).
[16] V. I. Ryzhii, R. A. Suris, and B. S. Shchamkhalova, Sov. Phys. Semicond. **20**, 1299 (1986).
[17] P. W. Anderson and W. F. Brinkman, cond-mat/0302129 (unpublished).
[18] A. A. Koulakov and M. E. Raikh, Phys. Rev. B **68**, 115324 (2003).
[19] A. V. Andreev, I. L. Aleiner, and A. J. Millis, Phys. Rev. Lett. **91**, 056803 (2003).
[20] A. C. Durst, S. Sachdev, N. Read, and S. M. Girvin, Phys. Rev. Lett. **91**, 086803 (2003).
[21] J. Shi and X. C. Xie, Phys. Rev. Lett. **91**, 086801 (2003).
[22] I. A. Dmitriev, A. D. Mirlin, and D. G. Polyakov, Phys. Rev. Lett. **91**, 226802 (2003).
[23] X. L. Lei and S. Y. Liu, Phys. Rev. Lett. **91**, 226805 (2003).
[24] X. L. Lei, J. Phys.: Condens. Matter **16**, 4045 (2004).
[25] V. Ryzhii and R. Suris, J. Phys.: Condens. Matter **15**, 6855 (2003).
[26] M. G. Vavilov and I. L. Aleiner, Phys. Rev. B **69**, 035303 (2004).
[27] S. A. Mikhailov, Phys. Rev. B **70**, 165311 (2004).
[28] J. Dietel, L. I. Glazman, F. W. J. Hekking, and F. von Oppen, Phys. Rev. B **71**, 045329 (2005).
[29] M. Torres and A. Kunold, Phys. Rev. B **71**, 115313 (2005).
[30] I. A. Dmitriev, M. G. Vavilov, I. L. Aleiner, A. D. Mirlin, and D. G. Polyakov, Phys. Rev. B **71**, 115316 (2005).
[31] J. Iñarrea and G. Platero, Phys. Rev. Lett. **94**, 016806 (2005).
[32] V. Ryzhii, cond-mat/0411370 (unpublished).
[33] C. Joas, J. Dietel, and F. von Oppen, cond-mat/0501397 (unpublished).
[34] C. S. Ting, S. C. Ying, and J. J. Quinn, Phys. Rev. B **14**, 5394 (1977).
[35] X. L. Lei and C. S. Ting, Phys. Rev. B **32**, 1112 (1985).
[36] X. L. Lei, J. L. Birman, and C. S. Ting, J. Appl. Phys. **58**, 2270 (1985).
[37] Associated with the elastic collision term in the Boltzmann equation for the distribution function is the momentum relaxation time or transport scattering time τ_m, which indicates an ability to collect particles along a preference direction such as the electric field or motion of c.m., thus inclined to deviate the system from the equilibrating distribution. The single-particle lifetime τ_s related to elastic scattering is the time that a quasiparticle can exist in a quantum state before it decays out. It represents an ability of spreading particles in all the directions, thus towards an isotropic distribution along an equal-energy ring. The equilibrating distribution is isotropic in the c.m. reference frame. The single-particle lifetime τ_s would not induce any deviation from an equilibrating-type distribution.
[38] X. L. Lei, J. Appl. Phys. **84**, 1396 (1998); J. Phys.: Condens. Matter **10**, 3201 (1998).
[39] X. L. Lei and S. Y. Liu, Appl. Phys. Lett. **82**, 3904 (2003).
[40] T. Ando, A. B. Fowler, and F. Stern, Rev. Mod. Phys. **54**, 437 (1982).
[41] M. E. Raikh and T. V. Shahbazyan, Phys. Rev. B **47**, 1522

(1993).
[42] K. W. Chiu, T. K. Lee, and J. J. Quinn *et al.*, Surf. Sci. **58**, 182 (1976).
[43] S. Y. Liu and X. L. Lei, J. Phys.: Condens. Matter **15**, 4411 (2003).
[44] Mulitiphoton ($|n|>1$) processes of course can take place in higher magnetic fields.
[45] V. Umansky, R. de Picciotto, and M. Heiblum, Appl. Phys. Lett. **71**, 683 (1997).
[46] X. L. Lei, cond-mat/0409219 (unpublished).